



BIDIRECTIONAL EV BIDIRECTIONAL BATTERY ADAPTER WITH VEHICLE-TO-GRID REACTIVE POWER

Busa Yerrinaidu^{1*}, R S R Krishnam Naidu²

Abstract—

The paper explores the integration of a grid connected off-board charger for Electric vehicle (EV) for reactive power compensation on grid side and synchronously used as a bidirectional electric vehicle battery charger (grid-to-vehicle (G2V)) and power generator (vehicle-to-grid (V2G)). A front-end with a grid facing bidirectional AC-DC cascade H-bridge converter makes up the topology of the charger, and a reversible back-end DC-DC adapter regulates the electricity flowing between the grid and the batteries of an electric car. As a safety precaution, the charger arrangement offers electrical separation between the consumer side and the remainder of the device by regulating battery current and EV current. Also, a controller with an adaptive notch filter is created for generating reference current synchronization and estimating system phase. Phase locked loops (PLL) are unused in the controller design with the recommended control algorithm. As outcome of enhanced steady-state and transient performance, the controller's computing complexity declines. Additionally, In the MATLAB/Simulink environment, a 12.6 kVA off-board adapter model is designed, additionally; how well the suggested control method performed is assessed during the G2V, V2G, and reactive power compensation operations of the EV adapter.

Keywords—Adaptive notch filter, EV Bidirectional Charger, Grid to vehicle, Vehicle to grid, Reactive power compensation

^{1*,2}Department of Electrical & Electronics Engineering, N S Raju Institute of Technology, Sontyam, Visakhapatnam -531173

***Corresponding Author:** Busa Yerrinaidu

*Department of Electrical & Electronics Engineering, N S Raju Institute of Technology, Sontyam, Visakhapatnam -531173

DOI: - 10.48047/ecb/2023.12.si10.00506

I. INTRODUCTION

EV's have received a lot of attention recently in industrialized community due to their lower petrol consumption and greenhouse gas emissions [1]. Off-board fast-charging station deployment is growing and one of the major drivers of the expanding use of EVs. Both unidirectional and bidirectional operation options are available for the off-board charger power electrical circuitry [2], [3]. G2V and V2G active power transfers are referred to as "bidirectional operation" V2G. Due to the EV batteries' ability to store energy, the V2G operation in the smart grid is exciting [3, 4]. There is still a problem with the EV batteries degrading during V2G usage. [5], [6] even though the grid's storage requirements may be met by the stored energy in EV batteries. On the other hand, employing chargers to provide additional services for power quality apart from the utilization of EV batteries with the grid preserves the battery's lifespan [5]. Due to their greater adaptability to power levels, off-board adapters are preferred to on-board adapters for achieving these additional functions [6].

The energy source delivers the reactive current in a typical power system. This impacts the system efficiency by adding new losses to the long transmission and distribution network's reactance. More voltage loss at the line reactance affects the system's voltage quality. It is therefore preferable to create local reactive load demand. In addition, household loads like compressors, refrigerators, washing machines, microwaves, and other smart gadgets consume the system's reactive power, which the customers don't pay enough for. In contrast, a reversible EV adapter can locally deliver reactive power without the need for more VAR compensators. This paper's primary objective is the operation of EV chargers as grid support. In order to increase the usage of EV's off-board charging stations with incorporated grid supplementary functions are installed in unused public spaces such as parking spaces, shopping malls, office blocks, residential properties, and restaurants.

The proposed EV adapter in [7] is intended to supply the grid's reactive power mitigation. EV batteries control the DC link voltage, which have an impact on its life, in order to ensure uninterrupted reactive power regulation. Additionally, it experiences more charge and discharge cycles, which shorten battery life. Reactive power regulation and further continuous functioning of the charger in G2V and V2G are not addressed. In a similar way, the charger is

utilized in [8] and [9] to meet the grid's reactive power needs. However, its efficiency and lifespan are decreased when EV batteries are utilized to regulate DC control voltage. In [10], [11], The EV adapter's reactive power adjustment operation in conjunction with the G2V operation is presented. While the proposed charger control technique does not include reactive power operation with V2G, using EV batteries, it controls the DC link. In [12], a multipurpose EV battery charger with reactive power compensation functions is presented. However, the study does not examine the charger's ability to operate in more than one operational mode simultaneously.

A two-way off-board EV battery adapter's development of an effective control strategy is discussed in this work in order to achieve reactive power correction as required by the grid. In addition to G2V or V2G working approach of the charger, reactive power correction is also possible with the suggested charger controller [15]. The V4G working mode is the name given to the charger's reactive power compensation mode in this paper. Galvanic isolation is another aspect of the suggested charger topology that makes the EV charger extremely reliable in real-world applications [16]. The UPF is maintained through charging by the EV charger controller. The suggested charger control technique removes PLL and includes an ANF to synchronize the grid. The controller now has better dynamics and less complicated implementation. In the control loop, direct power control is also used to provide a quick, dynamic response to a shift in power control. The charger performs better in steady-state conditions when ANF is used rather than PLL. The DC link voltage control term keeps the DC voltage link at its initial value is introduced to the inner current control loop.

The paper is structured as follows. The battery adapter is described in part-II. A comprehensive control technique is employed in this work is presented in part-III. The simulation outcomes are discussed in part-IV, and the paper is accomplished in part-V.

II. BIDIRECTIONAL OFF-BOARD EV BATTERY ADAPTER

Figure 1 shows the model arrangement for off-board EV battery charging. The designed EV charger is used to verify the charger's ability to compensate for reactive power as well as whether it operates in G2V or V2G mode. A single excited voltage source converter makes up the grid facing front-end AC-DC (CHBDC).

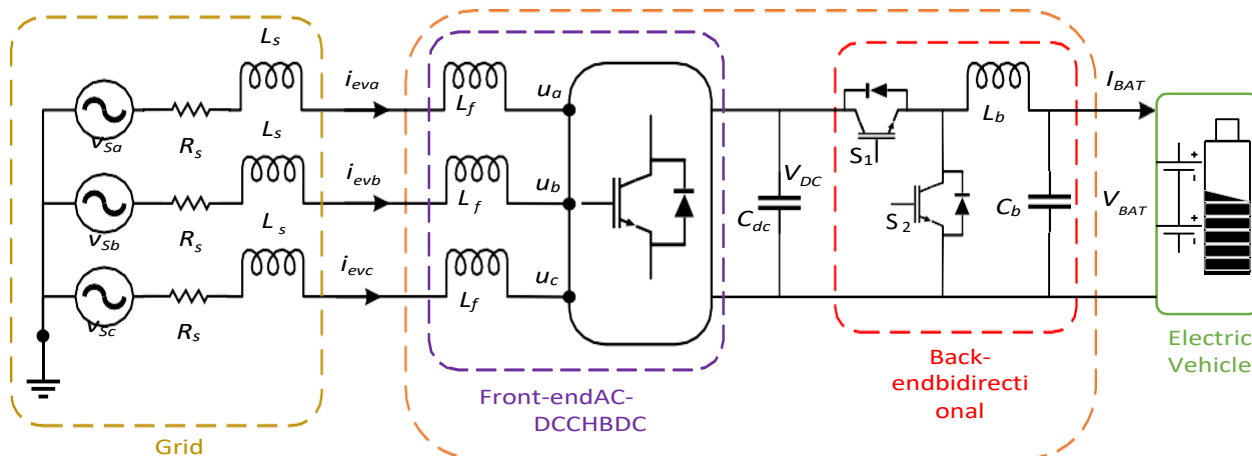


Fig.1.EV charger configuration

Figure 2 shows the grid facing converter's exact circuit arrangement. Three H-bridge sections are used in each phase of the converter in the arrangement that is being shown. A single-phase transformer's primary side is connected to every H-bridge output. In order to provide the per-phase output voltage, the secondary windings of three transformers are connected in series. According to Figure 2, every H-bridge produces up exactly 33.33% of the output voltage for each phase. Although toroidal transformers are used in front-end converters as a high-frequency connection, their use at the output side enhances their efficiency compared to prototypes using traditional transformer [13]. It also gets rid of the extra voltage matching sensors that were needed to keep the modules' power distribution balanced [13]. The additional benefits of the proposed H-bridge topology are galvanic isolation, minimized

charging current ripples, as well as capability for controlling voltage and current [13]. To enhance the output voltage of converter, Through the L-filter, the grid-facing CHBDC is connected to the electricity grid as illustrated in Fig. 1. L-filters are effective in eliminating higher-order switching harmonics because of their multilayer structure. In electric vehicles, the batteries are stored and drained using a DC-DC converter Fig. 1 depicts the BBDC's exact circuit configuration. By changing the two switches (S1, S2), the setup can be used in either of two operating modes (Buck or Boost). Switch S1 controls the BBDC to work as a buck converter, while switch S2 controls the BBDC to run in boost mode. Therefore, by running the BBDC in buck and boost modes, the electric vehicle batteries may be recharged and depleted.

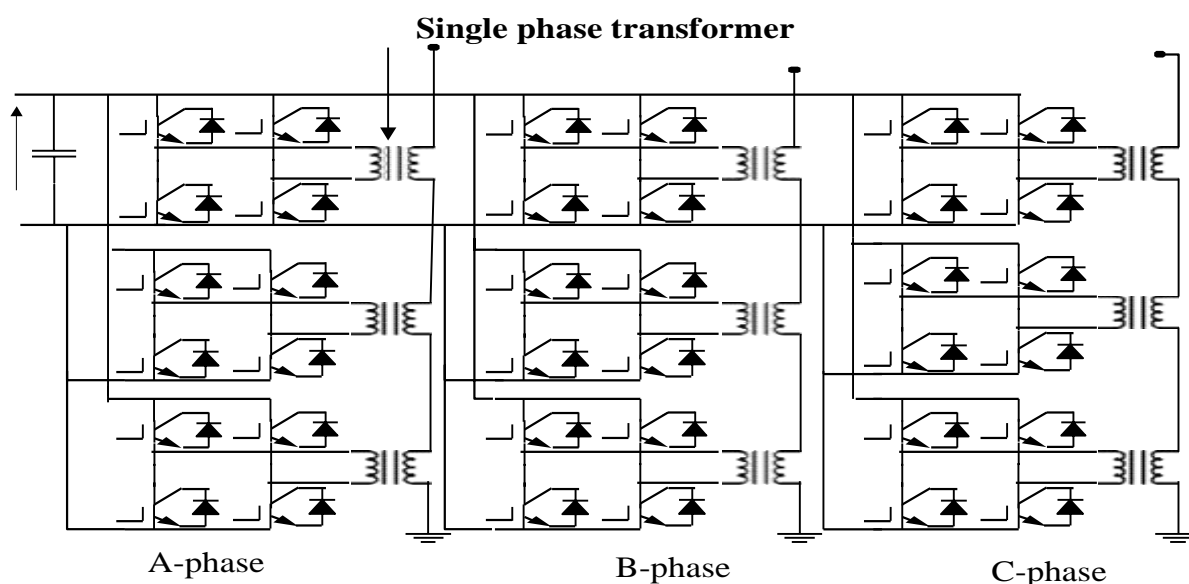


Fig. 2. CHBDC Circuit configuration

III. CONTROL STRATEGY OF THE EV ADAPTER

The converter created here works to serve two purposes in particular. Firstly, active power from the grid is used to charge the EV battery (G2V), and second, active power is returned to the grid when it is needed (V2G operation). Second, in response to a request from the utility grid operator, it supplies reactive electricity to the grid. The feature converter architecture is shown in Figure

3. The grid and the charger are kept in synchronization by the proposed control technique using ANF. The ANF for synchronization of grid was initially suggested in [14]. The ANF replaces conventional PLL in the system controller and operates efficiently despite system interruptions. Below is a list of the dynamic formulas for the ANF that can be stated as in [14].

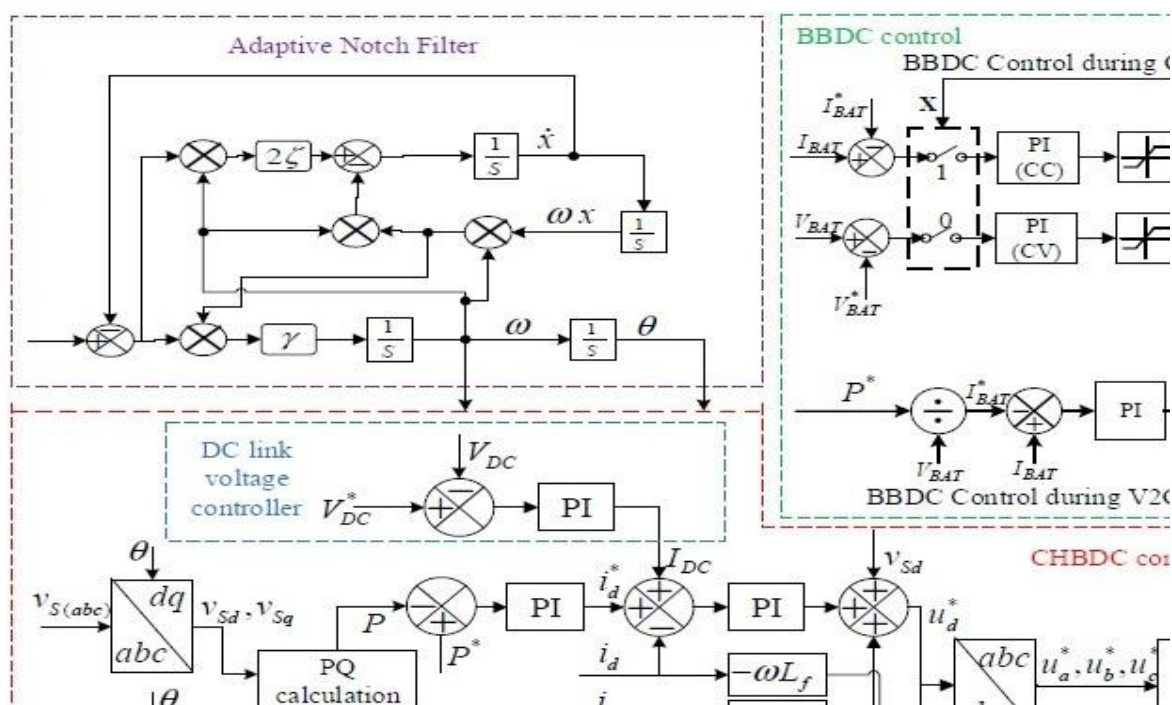


Fig. 3. Block diagram of bidirectional EV adapter

$$\begin{aligned} \dot{x} + \omega^2 x &= 2\zeta(t) \\ \dot{\omega} &= -\gamma x \omega e(t) \\ (t) &= (t) - x \end{aligned} \quad (1)$$

Where (t) is the input signal, ω is the estimated frequency of the input signal. The selection ζ and γ determine the ANF's estimation speed and accuracy. For primary frequency ω_1 with amplitude U_1 the ANF has a special periodic orbit at [14]:

$$\begin{pmatrix} x \\ \dot{x} \\ \omega \end{pmatrix} = \begin{pmatrix} -\frac{\zeta}{\omega_1} \cos(\omega_1 t + \varphi_1) \\ U_1 \sin(\omega_1 t + \varphi_1) \\ \omega_1 \end{pmatrix} \quad (2)$$

In order to determine the phase angle and frequency from the a-phase grid voltage V_{SA} , the detailed ANF construction is shown in Fig. 3. Park transformation is used to transfer the 3-phase grid currents and voltages from the abc-frame to the dq-frame as described in (3).

$$\begin{bmatrix} v_{sd} \\ v_{sq} \end{bmatrix} = [T] \begin{bmatrix} v_{sa} \\ v_{sb} \\ v_{sc} \end{bmatrix} \quad (3)$$

Where

$$[T] = \sqrt{\frac{2}{3}} \begin{bmatrix} \sin \theta & \sin(\theta - 2\pi/3) & \sin(\theta + 2\pi/3) \\ \cos \theta & \cos(\theta - 2\pi/3) & \cos(\theta + 2\pi/3) \end{bmatrix}$$

A three-phase source current's equivalent dq-frame transformation can also be calculated using the transformation matrix [T] provided in (3).

$$\begin{bmatrix} i_{sd} \\ i_{sq} \end{bmatrix} = [T] \begin{bmatrix} i_{sa} \\ i_{sb} \\ i_{sc} \end{bmatrix} \quad (4)$$

With this, (3) and (4) are used to calculate the instantaneous active and reactive power

$$\begin{aligned} P &= 3/2(v_{sd}i_d + v_{sq}i_q) \\ Q &= 3/2(v_{sq}i_q - v_{sd}i_d) \end{aligned} \quad (5)$$

Comparisons are made between the measured active and reactive power estimations extracted as of equation (5) and the reference active power (P^*) and reactive power (Q^*). In order to estimate reference active current (i_d^*) and reactive current (i_q^*), the error signal is transmitted through a PI controller as illustrated in Figure 3. The P^* command is the active power signal used to supply or charge a battery. The positive P^* symbol denotes the grid power that the charger must use for charging, while the negative symbol denotes the battery's active power that is sent to the grid. The Q^* shows how much reactive power the grid needs from the adapter. The adapter is asking the grid for reactive power because it needs inductive reactive power, which is

represented by positive Q^* . Negative Q^* is the capacitive reactive power that the grid requests from the adapter, and the adapter responds by supplying reactive power to the grid. To calculate the total active current component, the output IDC of the DC voltage link controller is combined with the active current component of the DC link voltage controller. The calculated grid current was then translated to the dq-frame utilizing the source active and reactive currents as a guide (4). To produce the reference voltage for CHBDC, the output of the inner PI control loop was initially added to the appropriate grid voltage that was measured in the dq-frame. The comprehensive computations are listed here:

$$\begin{aligned} u_d^* &= u_d + v_{sd} + \omega L_f i_q \\ u_q^* &= u_q + v_{sq} - \omega L_f i_d \end{aligned} \quad (6)$$

The adapter indicating voltage in the abc-frame is obtained by applying the inverse park transformation to the adapter indicating voltage in the dq-frame. Given in is the inverse transformation matrix (7).

$$[T]^{-1} = \sqrt{\frac{2}{3}} \begin{bmatrix} \sin \theta & \cos \theta \\ \sin(\theta - 2\pi/3) & \cos(\theta - 2\pi/3) \\ \sin(\theta + 2\pi/3) & \cos(\theta + 2\pi/3) \end{bmatrix} \quad (7)$$

As illustrated in Fig. 3, the space vector modulation receives the reference voltage for the charger as well as the real adapter voltage to produce the triggering pulses for the CHBDC. Besides the charger's recognized G2V and V2G operational modes. The adapter set-up and converter are intended to work in V4G mode

either separately or concurrently with G2V or V2G mode. Four charger working modes—G2V, V2G, G2V with V4G, and V2G with V4G—are examined and evaluated in this paper. Additionally, the charger controller makes it possible for the grid to receive together inductive and capacitive reactive power assistance when

running in V4G mode.

A. Grid to Vehicle (G2V)

The adapter uses the grid to provide the necessary active charging power to charge the batteries when operating in G2V state. This study employs the constant voltage (CV) and constant current (CC) approach for battery storing. In the first storing phase, the stored current is adjusted to the appropriate power point and maintained there awaiting the battery voltage reaches the manufacturers acceptable voltage level [17]. After that, the battery is stored with a decreasing current at a maximum voltage level until the battery voltage exceeds its maximum level and the current passes its rated cutoff point. In this operational state, the CHBDC control function maintains UPF at its input while following to the charging power command P^* . Reactive power command Q^* is equal to 0 in this operating state. The BBDC performs as a buck converter by managing the switching of S1 to manage the voltage (V_{BAT}) and battery storing current (I_{BAT}) during charging. Fig. 3 shows the BBDC controller topology during the G2V operation. The same variables are used in Figure 1 as well.

B. Vehicle to grid (V2G)

The EV adapter operates using V2G sends power through the battery to the electrical grid. G2V process is the charger's main purpose whenever an EV is connected to the grid. Both directions of power flow could be achievable for a while, with the incorporation of a BBDC [18]. Power is transmitted to the grid from the batteries as necessary to meet the needs of the electrical grid and for the comfort of EV buyers. By configuring the reference power control P^* to be negative data and Q^* to equal 0, throughout this stage, the CHBDC is adjusted to keep a 180° phase difference between EV current and grid voltage. The reference current generation time command and reference power P^* are supplied to the EV charger control algorithm. Equation 8 can be used to estimate the reference battery

current (I_{BAT}^*) while ignoring power losses associated with EV chargers.

$$I_{BAT}^* = \frac{P^*}{V_{BAT}} \quad (8)$$

C. G2V with V4G BAT V BAT

The EV charger works in this method when both the EV batteries are being stored and the grid is in need of reactive power support. The controller for the adapter allows grid support for together inductive and capacitive reactive power [19]. When operating, the positive sign of the power control P^* is used to support inductive reactive power when charging batteries, and the negative signal of the power command Q^* is used to support capacitive reactive power. In Figure 3, the CHBDC controller manages switching of the CHBDC to meet the necessary power demand after receiving the appropriate power order. The S1 as in G2V mode switch to store the battery is managed by the BBDC.

D. V2G with V4G

When the grid requires reactive power assistance, the EV charger also draws energy from the batteries when it is operating in this mode [20]. The charger controller enables grid reactive power support for both inductive and capacitive systems [21]. In this operating mode, the power command P^* always has a real number with a negative value. When a battery is being discharged, the optimistic signal of the power control Q^* denotes support for inductive reactive power, and the negative signal of Q^* denotes capacitive reactive power. When the appropriate power order is received, the CHBDC controller in Fig. 3 regulates the conversion of CHBDC to meet the necessary power condition. To discharge the battery, S2 is switched on and off by the BBDC.

Table-I Specified simulation parameter values

Parameters	Specifications
Charger apparent power	12.6 kVA
CHBDC Filter	$L_f=2.5$ mH (25A)
BBDC elements	$L_b=3.7$ mH, $C_b = 660$ μF
Grid Impedance (Z_s)	$R_s=0.1$ Ω , $L_s=1.6$ mH,
DC link Capacitor(CDC)	2200 $\mu F/500$ V
Transformer (CHBDC)	1kVA, 1- ϕ , Toroidal core
Supply System	230 Vrms, 50 Hz
EV Battery	Nominal voltage= 192 V,

IV. RESULTS AND DISCUSSION

To assess how well the suggested EV battery charger controller performs in the charger's designated function, a MATLAB/Simulink design is created. Table-I is a list of the simulation design variables used in this research. The charger's operation begins by storing the battery in G2V operating mode, with the understanding that it will provide reactive power at any time from the utility grid. If the grid wants reactive power, it enables the converter to operate with a

varied charging power. Fig. 4 shows the adapter's work during a $P^*=12$ kW charging session. Fig. 4 displays the three charger voltages (u), electric vehicle currents (iev), electric vehicle output power (Pev), electric vehicle output reactive power (Qev), and DC link voltage (VDC). The outcomes demonstrate that the EV power Pev arrives after the active power command P^* . As Q^* is set to Zero, the EV current and voltage are in phase.

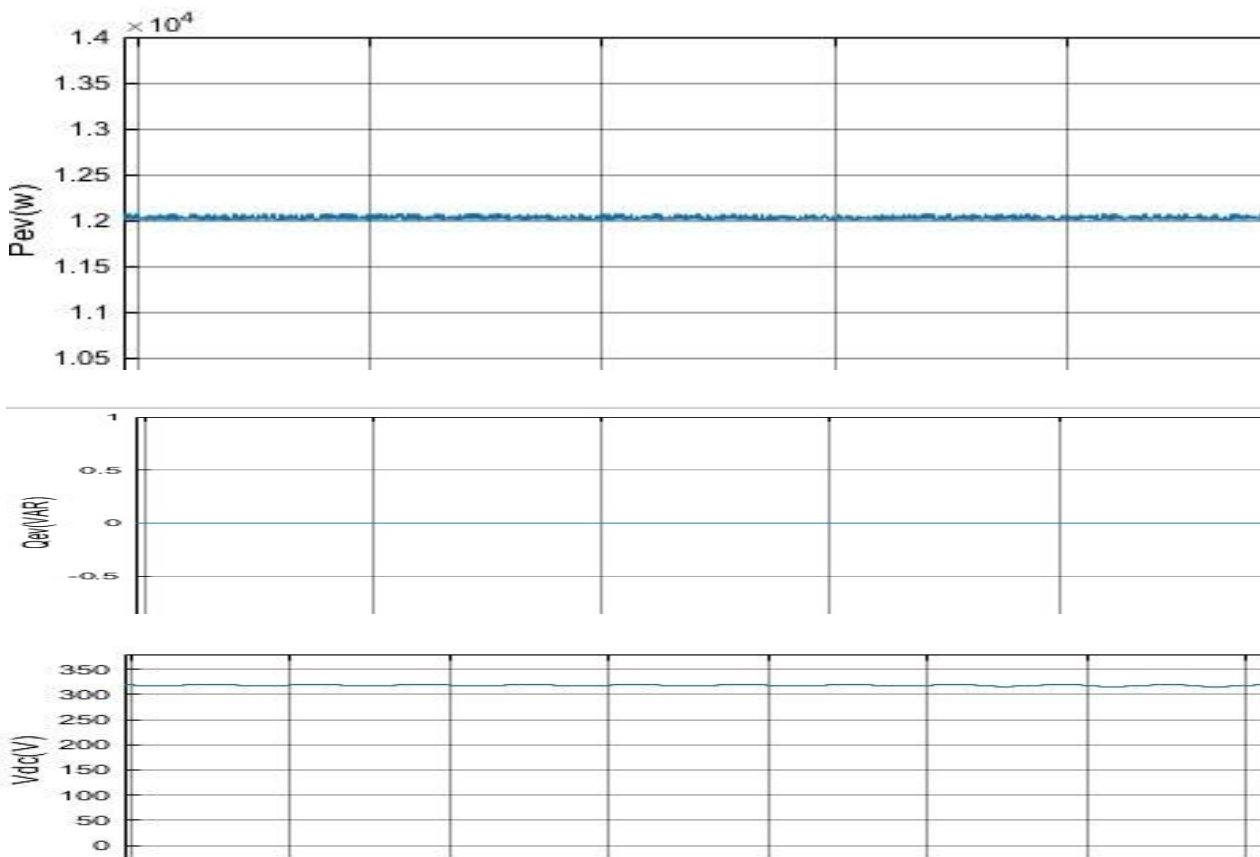


Fig. 4. Performance of EV chargers in G2V mode

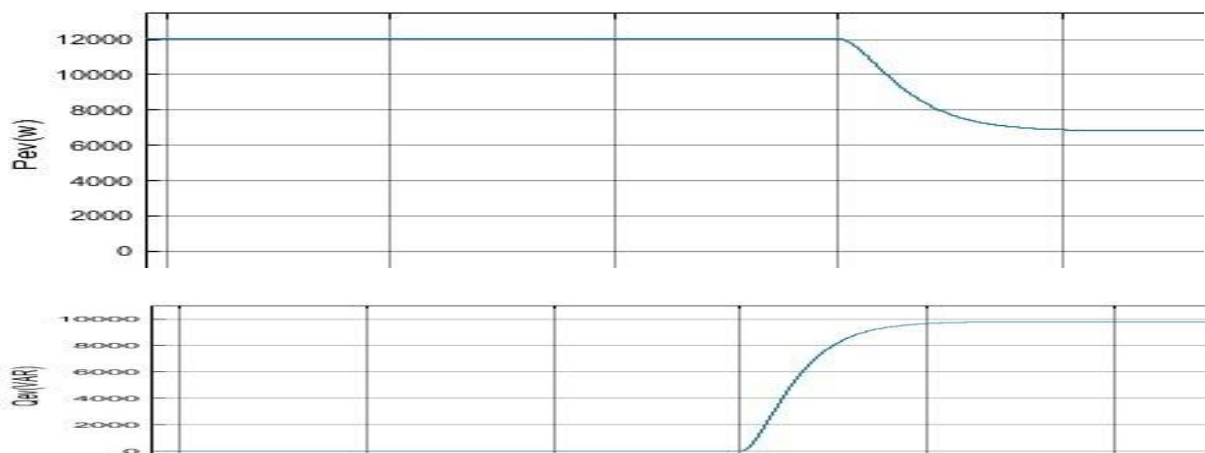




Fig. 5. Changing from G2V to G2V with V4G (inductive reactive power).

The grid changes the charger's operating state from G2V to G2V with V4G when charging at 1.5 secs, thus you must ask the charger for inductive reactive power. The grid has been given the power commands $Q^* = 9.8$ kVAR and $P^* = 6.8$ kW. Fig. 5 shows the change from G2V mode to G2V with V4G operating with inductive reactive power requirement. The reference power commands P and Q are followed by the EV power output P_{ev} and Q_{ev} , which settles in less than two grid cycles. At this moment, the DC link voltage overshoots and then returns to its reference point. The EV current and EV voltage are in phase before the change, however, following the transition, the EV current begins to trail the EV voltage. The EV current's amplitude stays constant since the adapter power is limited to its

rated value during the transition. The grid requires charging device capacitive reactive power with $Q^* = -9$ kVAR and $P = 8$ kW during operation at 3.5 s. As a result, the charger's inductive reactive power demand is changed to capacitive reactive power demand.

Figure 6 illustrates the adapter's operation after receiving this power command. After the adjustment, as expected, the lagging EV current shifts to leading the EV voltage. The DC link voltage dropped during the transition and returned to its predetermined level in a maximum of two cycles. The magnitude of the EV current stays constant since the power of the charger will be limited at its maximum rating during the transition.

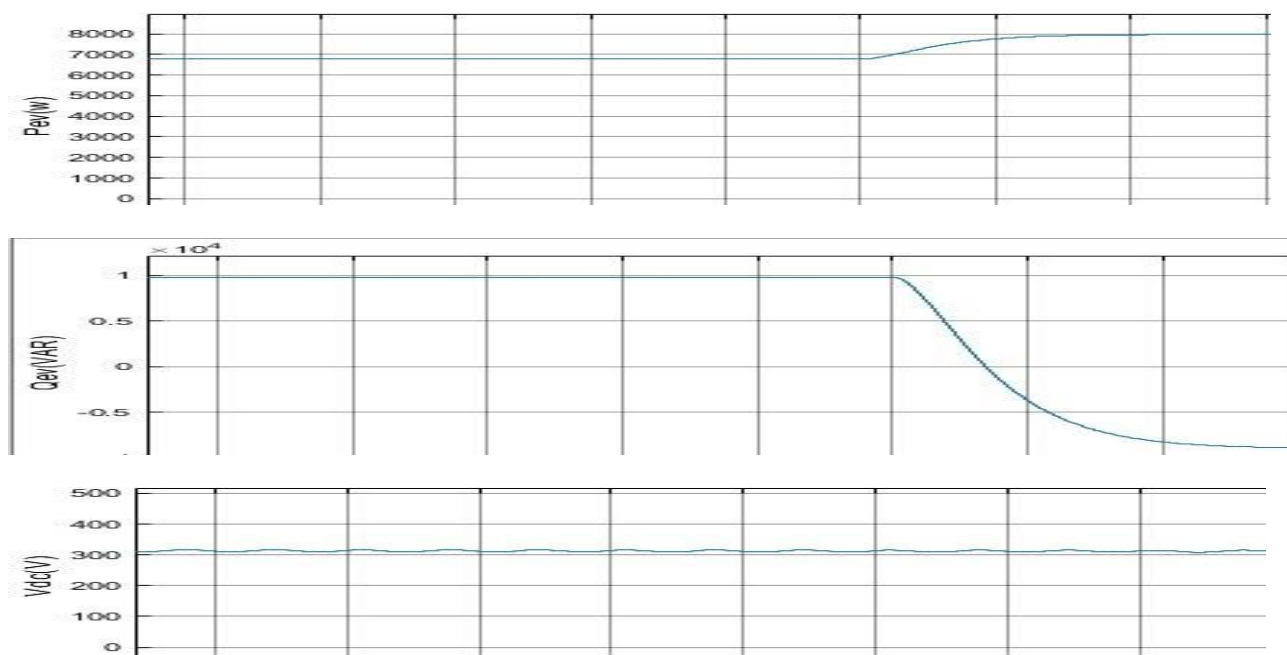
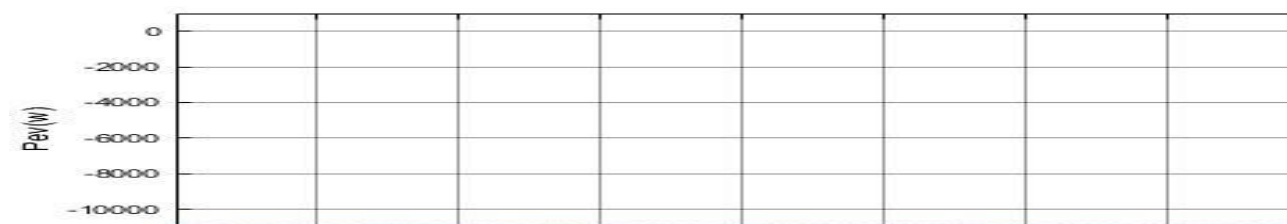


Fig. 6. Changing from inductive to capacitive reactive power operating modes (G2V with V4G).



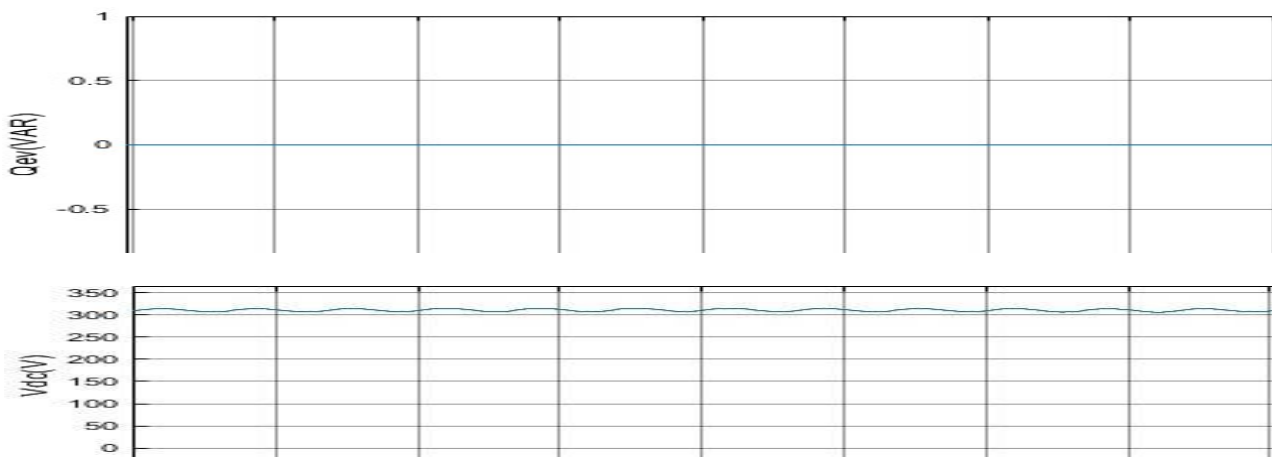


Fig. 7. Performance of EV chargers in V2G mode.

Fig. 7 illustrates the charger's performance while it is in the V2G working mode. $P^* = -11$ kW is the reference active power setting. Fig. 8 shows how the operating mode of the charger switches power command from V2G to V2G while using V4G operation $Q^* = 9$ kVAR and $P^* = -6.3$ kW. To meet the demand for grid power, the

associated electrical quantities are changed in response to changes in power commands. Fig. 9 demonstrates how reactive power command has changed from inductive to capacitive with $Q^* = -6.7$ kVAR and $P^* = -8.7$ kW. The outcomes reflect the anticipated changes in the charger current.

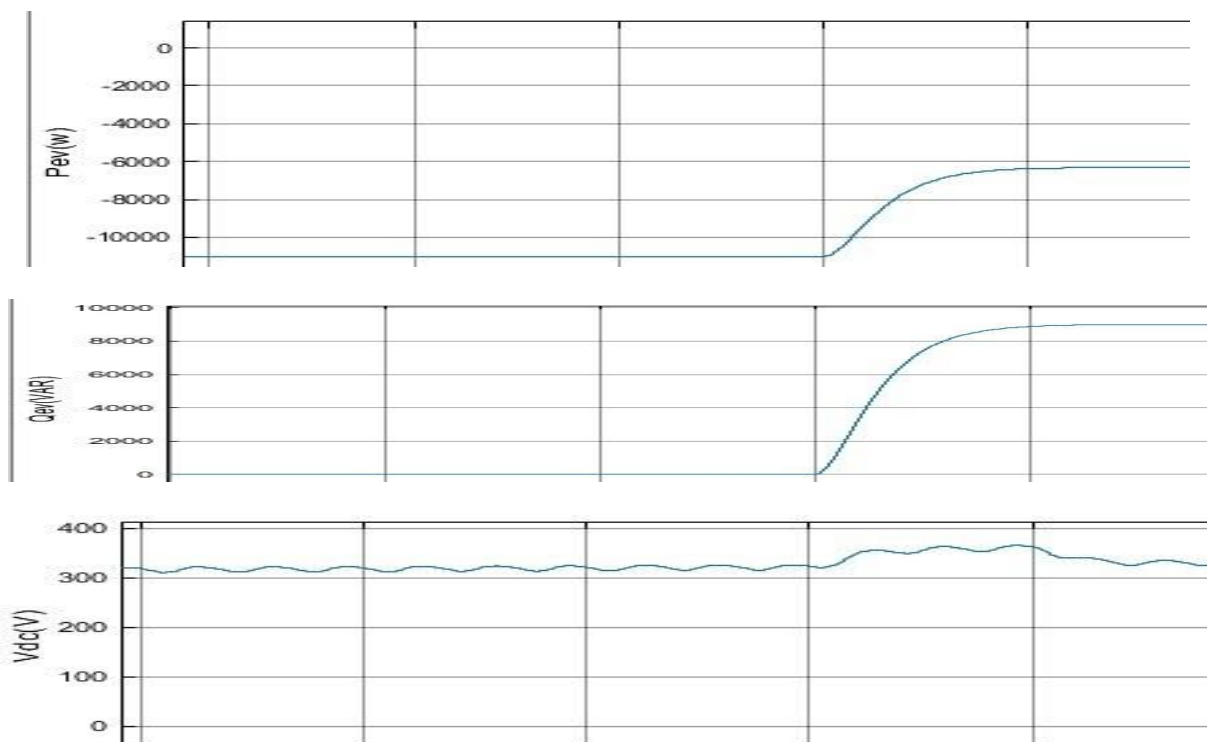
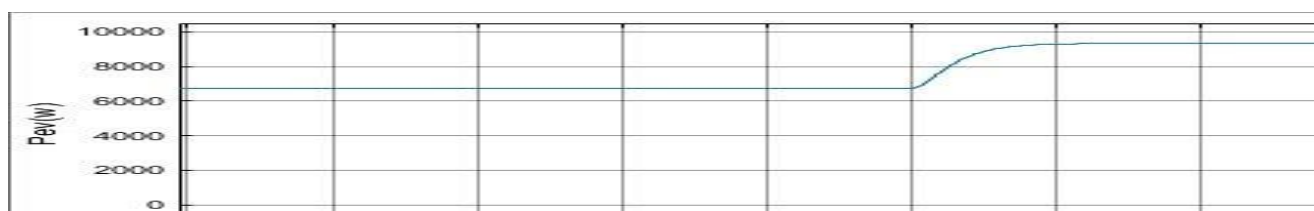


Fig. 8. Changing from V2G to V2G with V4G (inductive reactive power).



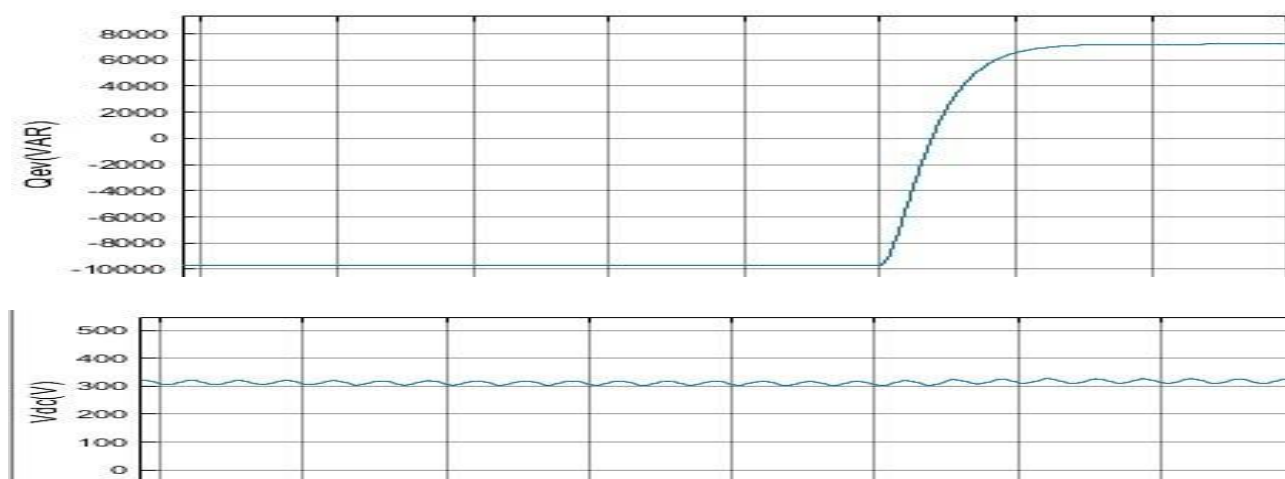


Fig. 9 changing from inductive to capacitive reactive power operating modes (V2G with V4G).

V. CONCLUSION

In this paper, an effective control technique that takes into account reactive power compensation, G2V and V2G mode, and EVs are proposed as a device that's active capable of storing, using, and producing power. Galvanic separation at the user end is provided by the charger arrangement as a security assess. The devised automation method performs admirably in various operating conditions, and the operational modes are successfully carried out after the power command. The charger works effectively in both stable-state and dynamic conditions. In less than two grid cycles, the off-board adapter reacts to the power command changeover. Reactive power operation doesn't have an impact on the EV batteries extending life. The simulation outcome under a variety of power command conditions, the suggested controller functions successfully. According to the results, the charger that is being offered is a strong contender to provide the utilities grid with support services for reactive power.

REFERENCES

- [1] S. S. Williamson, A. K. Rathore and F. Musavi, "Industrial Electronics for Electric Transportation: Current State-of-the-Art and Future Challenges," in *IEEE Transactions on Industrial Electronics*, vol. 62, no. 5, pp. 3021-3032, May 2015.
- [2] A. Kuperman, U. Levy, J. Goren, A. Zafransky, and A. Savernin, "Battery charger for electric vehicle traction battery switchstation," *IEEE Trans. Ind. Electron.*, vol. 60, no. 12, pp. 5391– 5399, 2013.
- [3] M. Restrepo, J. Morris, M. Kazerani and C. A. Canizares, "Modeling and Testing of a Bidirectional Smart Charger for Distribution System EV Integration," *IEEE Transactions on Smart Grid*, vol. 9, no. 1, pp.152-162, Jan. 2018.
- [4] A. Khaligh and S. Dusmez, "Comprehensive Topological Analysis of Conductive and Inductive Charging Solutions for Plug-In Electric Vehicles," *IEEE Transactions on Vehicular Technology*, vol. 61, no.8, pp. 3475-3489, Oct. 2012.
- [5] S. E. Letendre and W. Kempton, "The V2G concept: a new model for power?" *Public Utilities Fortnightly*, pp. 16–26, Feb. 2002.
- [6] M. Yilmaz and P. T. Krein, "Review of the impact of vehicle-to-grid technologies on distribution systems and utility interfaces," *IEEE Trans. Power Electron.*, vol. 28, no. 12, pp. 5573–5689, Dec. 2013.
- [7] M. Nikkhah Mojdehi and P. Ghosh, "An On-Demand Compensation Function for an EV as a Reactive Power Service Provider," in *IEEE Transactions on Vehicular Technology*, vol. 65, no. 6, pp. 4572-4583, June 2016.
- [8] Buja, M. Bertoluzzo and C. Fontana, "Reactive Power Compensation Capabilities of V2G- Enabled Electric Vehicles," *IEEE Trans, Power Electronics*, vol. 32, no. 12, pp. 9447-9459, Dec. 2017
- [9] D. B. Wickramasinghe Abeywardana, P. Acuna, B. Hredzak, R. P. Aguilera and V. G. Agelidis, "Single-Phase Boost Inverter-Based Electric Vehicle Charger With Integrated Vehicle to Grid Reactive Power Compensation," *IEEE Transactions on Power Electronics*, vol. 33, no. 4, pp. 3462-3471, April 2018.
- [10] M. Nikkhah Mojdehi and P. Ghosh, "An On-Demand Compensation Function for an EV as a Reactive Power Service Provider," *IEEE Trans. Vehicular Technol.*, vol. 65, no. 6, pp. 4572- 4583, June 2016.

- [11] G. Buja, M. Bertoluzzo and C. Fontana, "Reactive Power Compensation Capabilities of V2G-Enabled Electric Vehicles," *IEEE Trans. Power Electronics*, vol. 32, no. 12, pp. 9447-9459, Dec. 2017.
- [12] A. Verma and B. Singh, "Multi-Objective Reconfigurable Three-Phase Off-Board Charger for EV," *IEEE Trans. on Ind. Applicat.*, vol. 55, no. 4, pp. 4192-4203, July-Aug. 2019.
- [13] A. R. Dash, A. K. Panda, R. K. Lenka and R. Patel, "Performance analysis of a multilevel inverter based shunt active filter with RTEMD control technique under ideal and non-ideal supply voltage conditions," *IET Gen. Trans. & Dis.*, vol. 13, no. 18, pp. 4037-4048, Sep. 2019.
- [14] M. Mojiri, M. Karimi-Ghartemani and A. Bakhshai, "Time-Domain Signal Analysis Using Adaptive Notch Filter," in *IEEE Transactions on Signal Processing*, vol. 55, no. 1, pp. 85-93, Jan. 2007
- [15] R. Babu, S. Raj, and B. R. V. Prasad, "A Review at the Utilization of Renewable Energy in an Agricultural Operation," *Biophys. Econ. Sustain.*, vol. 6, no. 4, pp. 1-13, 2021, doi: 10.1007/s41247-021-00092-9.
- [16] BUGATHA RAM VARA PRASAD, C. PRASANTHI, G. JYOTHIKA SANTHOSHINI, K. J. S. V. KRANTI KUMAR, and K. YERNAIDU, "Smart Electrical Vehicle," *i-manager's J. Digit. Signal Process.*, vol. 8, no. 1, p. 7, 2020, doi: 10.26634/jdp.8.1.17347.
- [17] Bugatha Ram Vara prasad and K. Aswini, "Design of Bidirectional Battery Charger for Electric Vehicle," *Int. J. Eng. Res. Technol.*, vol. 10, no. 7, pp. 410-415, 2021, doi: 10.1088/1757-899x/1055/1/012141.
- [18] Bugatha Ram Vara prasad, "Solar Wireless Electric Vehicle Charging System," *Interantional J. Sci. Res. Eng. Manag.*, vol. 06, no. 06, pp. 1-7, 2022, doi: 10.55041/ijrsrem14449.
- [19] Bugatha Ram Vara prasad, "Design and Analysis of Bidirectional Battery Charger with Grid-to-Vehicle, Vehicle-to-Grid and Vehicle-to-Home Technologies," *Interantional J. Sci. Res. Eng. Manag.*, vol. 06, no. 06, pp. 1-8, 2022, doi: 10.55041/ijrsrem14407.
- [20] Bugatha Ram Vara prasad T.deepthi n.satyavathi v.satish varma r.hema kumar, "Solar charging station for electric vehicles," *Int. J. Adv. Res. Sci. Commun. Technol.*, vol. 7, no. 2, pp. 316-325, 2021, doi: 10.48175/IJARST-1752.
- [21] Prasad, B.R.V., Sai, B.S., Vijaychandra, J., Babu, R. (2023). Application of Renewable Energy in Charging Station for Electric Vehicles: A Comprehensive Review. In: Namrata, K., Priyadarshi, N., Bansal, R.C., Kumar, J. (eds) Smart Energy and Advancement in Power Technologies. Lecture Notes in Electrical Engineering, vol 927. Springer, Singapore. https://doi.org/10.1007/978-981-19-4975-3_18